Clinical and Experimental Immunology, 2024, **215**, 137–147
https://doi.org/10.1093/cei/uxad107
Advance access publication 14 September 2023
Research Article

Clinical & Experimental IMMUNOLOGY

OXFORD

Research Article

IL-21, not IL-17A, exacerbates murine primary biliary cholangitis

Chun-Wen Chan[1], Hung-Wen Chen[1], Yu-Wen Wang[1], Chia-I Lin[1], and Ya-Hui Chuang[*,1,2,]

[1]Department of Clinical Laboratory Sciences and Medical Biotechnology, College of Medicine, National Taiwan University, Taipei, Taiwan
[2]Department of Laboratory Medicine, National Taiwan University Hospital, Taipei, Taiwan

[*]Correspondence: Ya-Hui Chuang, PhD, Department of Clinical Laboratory Sciences and Medical Biotechnology, College of Medicine, National Taiwan University. No. 1, Chang-Te Street, Taipei, Taiwan. Email: yahuichuang@ntu.edu.tw

Abstract

Primary biliary cholangitis (PBC) is a chronic autoimmune liver disease caused by intrahepatic bile duct injuries, resulting in fibrosis, cirrhosis, and eventually liver failure. T helper (Th) 17 cells are proposed to involve in the pathogenesis of PBC. However, how and which Th17 cell-derived cytokines affect PBC remains unclear. In this study, we investigated the effects of Th17 effector cytokines, including interleukin (IL)-17A, IL-17F, and IL-21 in PBC using a xenobiotic-induced mouse model of autoimmune cholangitis (inducible chemical xenobiotic models of PBC) treated with cytokine-expressing adeno-associated virus. Our results showed that administration of IL-17A, the well-known main cytokine produced by Th17 cells, did not augment liver inflammation or fibrosis. In contrast, we noted IL-17A-treated mice had lower hepatic Th1 cell numbers and higher hepatic $CD11b^+Ly6G^+$ polymorphonuclear myeloid-derived suppressor cell numbers. IL-17F did not alter liver inflammation or fibrosis. However, the administration of IL-21 exacerbated liver inflammatory responses and portal cell infiltration. IL-21 markedly increased the numbers of activated $CD8^+$ T cells and liver tissue-resident memory $CD8^+$ T cells. Moreover, IL-21 aggravates liver fibrosis in mice with autoimmune cholangitis. These results emphasized that not IL-17A but IL-21 in Th17 cell-derived cytokines affected the pathogenesis of PBC. IL-21 enhanced liver inflammation and progression to fibrosis by enhancing the numbers and effector activities of $CD8^+$ T cells. Delineation of the effects of different Th17 effector cytokines in PBC offers clues for developing new therapeutic approaches.

Keywords: autoimmune disease, Th17, interleukin-17A, interleukin-17F, interleukin-21, tissue-resident memory T cell

Abbreviations: 2-OA-OVA: 2-octynoic acid (2-OA) coupled with ovalbumin; α-SMA: α-smooth muscle actin; AAV: adeno-associated virus; AMA: anti-mitochondrial autoantibody; HSC: hepatic stellate cell; MDSC: myeloid-derived suppressor cell; PBC: primary biliary cholangitis; PDC-E2: E2 component of the pyruvate dehydrogenase complex; Tcm: central memory T; Tem: effector-memory T; Trm: tissue-resident memory T.

Introduction

Primary biliary cholangitis (PBC) is a progressive, autoimmune liver disease. It is characterized by the presence of disease-specific anti-mitochondrial autoantibodies (AMAs) and autoreactive $CD4^+$ and $CD8^+$ T cells specific to the E2 component of the pyruvate dehydrogenase complex (PDC-E2). The destruction of biliary epithelial cells, the targets of PBC, is mediated by liver-infiltrating $CD4^+$ and $CD8^+$ T cells [1, 2].

T helper 17 (Th17) cells are a subtype of activated $CD4^+$ T cells defined by their dominant interleukin (IL)-17 production. Th17 cells mediate host–defense mechanisms against various infections, especially extracellular pathogens and fungal infections and the pathogenesis of many autoimmune diseases via the production of several effector cytokines, including IL-17A, IL-17F, IL-21, and IL-22 [3, 4]. In PBC, IL-17-producing cells accumulate around damaged bile ducts in patients' specimens [5–7]. Biliary epithelial cells can produce Th17-inducible cytokines, IL-6, IL-1β, and IL-23 when stimulated with pathogen-associated molecular patterns [5]. Expression of Th17-related cytokines IL-1β, IL-6, IL-23, and IL-17 are upregulated in serum and peripheral blood mononuclear cells from patients with PBC compared with those of healthy subjects [8]. In addition, advanced PBC patients present more Th17 cells in the liver than early PBC patients [7, 9]. These results suggest that Th17 cells are involved in the pathogenesis of PBC. However, which cytokines derived from Th17 cells are effector ones and how the effector cytokines work in the pathogenesis of PBC remain unclear.

IL-17A is the main cytokine produced by Th17 cells. IL-17A and IL-17F are members of the IL-17 family. They are genetically linked and highly homologous, with 50% amino acid identity. They form a heterodimer and bind to the same receptor, the IL-17 receptor A (IL-17RA)-IL-17RC; however, IL-17A binds IL-17RA with much higher affinity [10]. IL-17A and IL-17F are chief cytokines that promote inflammation by increasing chemokine production in tissues to recruit monocytes and neutrophils to the injured tissue [3]. IL-17A and/or IL-17F are responsible for developing many autoimmune diseases, such as rheumatoid arthritis, psoriasis, and juvenile idiopathic arthritis [11–13]. IL-17A is also involved in organ fibrosis [14–16].

Received 29 June 2023; Revised 23 August 2023; Accepted for publication 13 September 2023

It enhances liver fibrosis through direct or indirect hepatic stellate cell (HSC) activation by inducing fibrogenic signals in them [16, 17].

IL-21 is an IL-2-family cytokine that mediates its functions via the IL-21 receptor broadly expressed in hematopoietic populations and epithelial cells [18]. IL-21 enhances the cytotoxic activity of $CD8^+$ T and NK cells, contributes to the functional differentiation of follicular helper T and Th17 cells, and drives the differentiation of B cells into memory cells and terminally differentiated plasma cells [19–21]. IL-21 is also involved in antitumor and antiviral responses and promotes the development of autoimmune and inflammatory disorders [18]. IL-22 is a member of the IL-10 cytokine family. IL-22 prevents hepatic injury and modulates inflammation in many autoimmune diseases [22]. Our previous study showed that the administration of IL-22 significantly reduced portal inflammatory responses and liver fibrosis in a mouse model of PBC [23].

To investigate the effects of Th17 effector cytokines, including IL-17A, IL-17F, and IL-21 in PBC, we treated the xenobiotic-induced mouse model of autoimmune cholangitis (inducible chemical xenobiotic models of PBC) with liver-preferred cytokine-expressing adeno-associated virus (AAV) and determined the autoimmune cholangitis features of diseased mice. Mice immunized with xenobiotics, 2-octynoic acid (2-OA) coupled with ovalbumin (2-OA-OVA) develop AMAs and autoimmune cholangitis with a significant increase in lymphocyte infiltrates, including $CD4^+$ and $CD8^+$ T cells, B cells, NK cells and NKT cells, portal inflammation, granuloma formation, and bile duct damage, which are similar to the features of human PBC [23–26]. Most importantly, in contrast to other gene-knockout mouse models, 2-OA-OVA-induced autoimmune cholangitis mice develop pathological and immunological features major in the liver [23–26]. In addition, our previous study showed that 2-OA-OVA-induced autoimmune cholangitis mice had apparent IL-17-expressing $CD4^+$ T cells in the liver [24], making 2-OA-OVA-induced autoimmune cholangitis mice an excellent model for studying Th17 effector cytokines in liver-specific autoimmune disease. However, the expression of IL-17 and IL-17-expressing $CD4^+$ T cells was moderate [24]; hence, we employed liver-preferred AAV-mediated overexpression of these cytokines to simulate the effects of Th17 cell-derived cytokines in the liver. Here, we demonstrated that administering IL-17A and IL-17F had little to no effect on liver inflammation and fibrosis in mice with autoimmune cholangitis. However, the administration of IL-21 markedly enhanced liver inflammation and liver fibrosis in autoimmune cholangitis. Hence, not IL-17A but IL-21 was the effector Th17 cell-derived cytokines mediated the pathogenesis of PBC. Delineation of the effector cytokines to PBC will help develop new therapeutic approaches.

Materials and methods

Preparation of adeno-associated virus-cytokine

AAV-IL-17A, AAV-IL-17F, and AAV-IL-21 were generated by a helper-free packaging system (AAV-DJ, Cell Biolabs, San Diego, CA, USA). AAV-DJ, a recombinant AAV produced by a complex library of hybrid capsids from eight different wild-type viruses, has a superior transduction efficiency in the liver [27]. Viral particles were purified and were quantified as previously reported [23–25]. AAV-mock is a control virus, which is identical but contains no transgene in the expression cassette.

Experimental mice and protocol

Female C57BL/6 mice aged 7–9 weeks were intraperitoneally immunized with 20 μg of 2-OA-OVA in the presence of complete Freund's adjuvant (CFA, Sigma–Aldrich, St. Louis, MO, USA) and subsequently boosted every 2 weeks with 2-OA-OVA in incomplete Freund's adjuvant (IFA, Sigma–Aldrich) [23–26, 28]. AAV-IL-17A, AAV-IL-17F, AAV-IL-21, and AAV-mock (1.5×10^9 TU/mouse) were intravenously injected into mice at 2 weeks after the first 2-OA-OVA immunization. Mice were sacrificed at 5 weeks postimmunization to analyze liver inflammation and the subsets and function of immune cells or at 11 weeks postimmunization for liver pathology examination, as described below. Mice were obtained from the National Laboratory Animal Center, Taiwan, and were maintained in the Animal Center of the College of Medicine, National Taiwan University. The animal study was approved by the Institutional Animal Care and Use Committee (IACUC) of the National Taiwan University College of Medicine and College of Public Health. All experiments were performed two to four times, each with a 3–5 mice group size.

Quantitative PCR

Total RNA from liver specimens was obtained using the TRI^{zol} (Invitrogen Life Technologies, Carlsbad, CA, USA) or Nucleospin RNA commercial kit (Macherey-Nagel, Düren, Germany) with DNA removal for the detection of cytokine expression in Fig. 2a. cDNA was synthesized using High-Capacity cDNA Reverse Transcription Kits (Applied Biosystems, Foster City, CA, USA), followed by real-time PCR analysis (SYBR green; Applied Biosystems). Primers were designed according to the published sequences and listed in Table 1. β-actin serves as an internal control. Relative quantification was performed using the comparative threshold cycle (C_T) method.

Quantitation and functional assay of liver mononuclear cells

Livers were perfused and dissociated with the gentleMACS Dissociator (Miltenyi Biotec, Auburn, CA, USA). After centrifugation at 50×*g* for 5 minutes, the parenchymal cells were removed as pellets. Leukocytes in the nonparenchymal cells were isolated using 40% and 70% Percoll (GE HealthCare Biosciences, Quebec, Canada). Subsets of liver mononuclear cells and functional assays of liver lymphocytes were conducted using flow cytometry. Before staining cells with a previously defined optimal dilution of monoclonal antibodies, the cells were preincubated with anti-CD16/32 (clone 93) to block non-specific FcRγ binding. The following mAbs were used in this study: anti-CD3 (clone 145-2C11), anti-CD4 (clone GK1.5), anti-CD8a (clone 53-6.7), anti-CD19 (clone 6D5), anti-NK1.1 (clone PK136), anti-CD69 (clone H1.2F3), anti-CD44 (clone IM7), anti-CD62L (clone MEL-14), anti-CD185 (CXCR5, clone L138D7), anti-IAb (clone AF6-120.1), anti-CD11b (clone M1/70), anti-CD11c (clone N418), anti-F4/80 (clone BM8), anti-Ly6C (HK1.4), anti-Ly6G (clone 1A8), anti-FasL (Biolegend, San Diego). For cytokines and granzyme B detection, liver mononuclear cells were stimulated with phorbol-myristate acetate (PMA, 50 ng/mL,

Table 1. List of primers for quantitative RT-PCR.

Gene name		Sequence
β-actin	Forward	5' CACAGTGTTGTCTGGTGGTA 3'
	Reverse	5' GACTCATCGTACTCCTGCTT 3'
IFN-γ	Forward	5' GGCCATCAGCAACAACATAAGC 3'
	Reverse	5' TGGACCACTCGGATGAGCTCA 3'
TNF-α	Forward	5' CCCCAAAGGGATGAGAAGTTC 3'
	Reverse	5' TGAGGGTCTGGGCCATAGAA 3'
CXCL9	Forward	5' ATTGTGTCTCAGAGATGGTGCTAATG 3'
	Reverse	5' TGAAATCCCATGGTCTCGAAAG 3'
CXCL10	Forward	5' GGATGGCTGTCCTAGCTCTG 3'
	Reverse	5' TGAGCTAGGGAGGACAAGGA 3'
α-SMA	Forward	5' TCCTCCCTGGAGAAGAGCTAC 3'
	Reverse	5' TATAGGTGGTTTCGTGGATGC 3'
IL-17A	Forward	5' AAGGCAGCAGCGATCATCC 3'
	Reverse	5' GGAACGGTTGAGGTAGTCTGA 3'
IL-17F	Forward	5' TGAATTCCAGAACCGCTCCA 3'
	Reverse	5' TTTCTTGCTGAATGGCGACG 3'
IL-21	Forward	5' GCCAGATCGCCTCCTGATTA 3'
	Reverse	5' CATGCTCACAGTGCCCCTTT 3'

Sigma–Aldrich) and ionomycin (1 μg/mL, Sigma–Aldrich) for 4 or 18 hours and IFN-γ, IL-17A, or granzyme B intracellular staining was performed after staining with cell surface molecules. Anti-IFN-γ (clone XMG1.2), anti-granzyme B (clone GB11), and IL-17A (clone TC11-18H10) (BD Biosciences, San Diego) were used. Stained cells were measured with a flow cytometer (Attune NxT Flow Cytometer, ThermoFisher Scientific) and analyzed using FlowJo software (Tree Star, Inc., Ashland, OR, USA). Zombie Fixable Viability Kit (Biolegend) was used in all experiments to exclude dead cells in flow cytometry analysis.

Determination of serum AMAs

Purified mouse recombinant PDC-E2 at 10 μg/mL in carbonate buffer (pH 9.6) was coated onto ELISA plates at 4°C overnight. After blocking with 1% casein (Sigma–Aldrich), diluted sera were added for 2 hours at room temperature. In parallel, one positive pool serum was diluted serially and added to each plate to constitute an internal standard. HRP-labeled anti-mouse IgG (Invitrogen, Camarillo, CA, USA) diluted 1/10 000 in blocking buffer was added to detect mouse antibodies. Optical density was read at 450 nm and 540 nm.

Western blot of α-smooth muscle actin

Protein samples in RIPA lysis buffer (Sigma) were heated at 95°C for 10 minutes and separated on SDS-polyacrylamide gel. Then proteins were electroblotted to polyvinylidene fluoride (PVDF) membranes and revealed by rabbit antibodies against α-SMA (1:1000, Abcam, Cambridge, UK) overnight at 4°C. Finally, according to the manufacturer's instructions, the blot was subjected to chemiluminescent detection. GAPDH (1:1000, Abcam) was the internal control. Quantitation was analyzed using ImageJ software.

Histopathology and immunohistochemistry of liver

Portions of the liver were excised and immediately fixed with a 10% buffered formalin solution for one day at room temperature. Paraffin-embedded tissue sections were then cut into 4–7 μm slices for routine hematoxylin and eosin (H&E) staining and Masson's trichrome staining. For immunohistochemistry, after deparaffinization and rehydration, 3 μm of FFPE tissue sections were submerged in Tris-EDTA Buffer (10mM Tris Base, 1mM EDTA Solution, 0.05% Tween 20, pH 9.0) to performed heat-induced antigen retrieval with an autoclave for 20 minutes. The tissue section was placed at room temperature to cool down and applied with blocking buffer (1% BSA, 0.3M glycine, 0.5% saponin in PBS) for 1 hour. For the staining of leukocytes, the slides were stained with unconjugated anti-CD45 Ab (diluted 1:250 in 1% BSA, clone EPR20033, Abcam) overnight at 4°C and detected by Alexa594 conjugated anti-rabbit IgG antibody (diluted 1:500 in 1% BSA, Abcam) for 40 minutes at room temperature. After counterstaining with DAPI, slides were observed by a fluorescence microscope (Olympus IX83). Quantitation of the percentages of CD45 positive signals in the liver was analyzed using ImageJ Fiji software by the positive fluorescence pixel over the total pixel in a visual field (magnification ×100) of the immunostained sections. The average of 30 randomly chosen fields was calculated.

Statistical analysis

Data are expressed as the mean ± standard error of the mean (SEM). A two-sided unpaired Student's *t*-test was used to determine significant differences between the two groups. Comparison of more than two groups was performed with one-way ANOVA followed by Dunnett's multiple comparison test. The Spearman test was used to evaluate correlations. Statistically significant differences were defined as *P*-values of less than 0.05, less than 0.01, less than 0.001, and less than 0.0001 (Prism 9; Graph-Pad Software, La Jolla, CA, USA).

Results

Effects of Th17 effector cytokines on autoimmune cholangitis

We immunized the mice with 2-OA-OVA to induce autoimmune cholangitis. Two weeks after the first 2-OA-OVA immunization, we intravenously treated them with liver-preferring AAV-IL-17A, AAV-IL-17F, AAV-IL-21, or AAV-mock. Pathological examination was performed 11 weeks post-immunization. *Il21*, *Il17A*, and *Il17F* mRNA were detected in the livers of AAV-IL-21-, AAV-IL-17A-, and AAV-IL-17F-treated mice, respectively (Fig. 1a). We observed cell infiltration in the portal area in all groups of mice. Still, there were no differences in the degree of infiltration among IL-17A, IL-17F, and mock groups. A marked increase in portal inflammation was observed in mice treated with IL-21 (Fig. 1b). Furthermore, we observed a more significant influx of $CD45^+$ leukocytes (shown in red) around the bile duct of IL-21-treated mice (Fig. 1c). Liver fibrosis in liver sections stained with Masson's trichrome was evident in mice treated with IL-21 (Fig. 1d). As expected, there was a higher expression of α-smooth muscle actin (α-SMA), an important marker of HSC activation to myofibroblast-like cells, in mice treated with IL-21 compared to the mock group. There were no differences in the expression levels of α-SMA among IL-17A, IL-17F, and mock groups (Fig. 1e and f).

Serum anti-PDC-E2 IgG and liver *Ifn-γ*, *Tnf-α*, and *Cxcl9* levels were not changed in mice treated with IL-17A or IL-17F

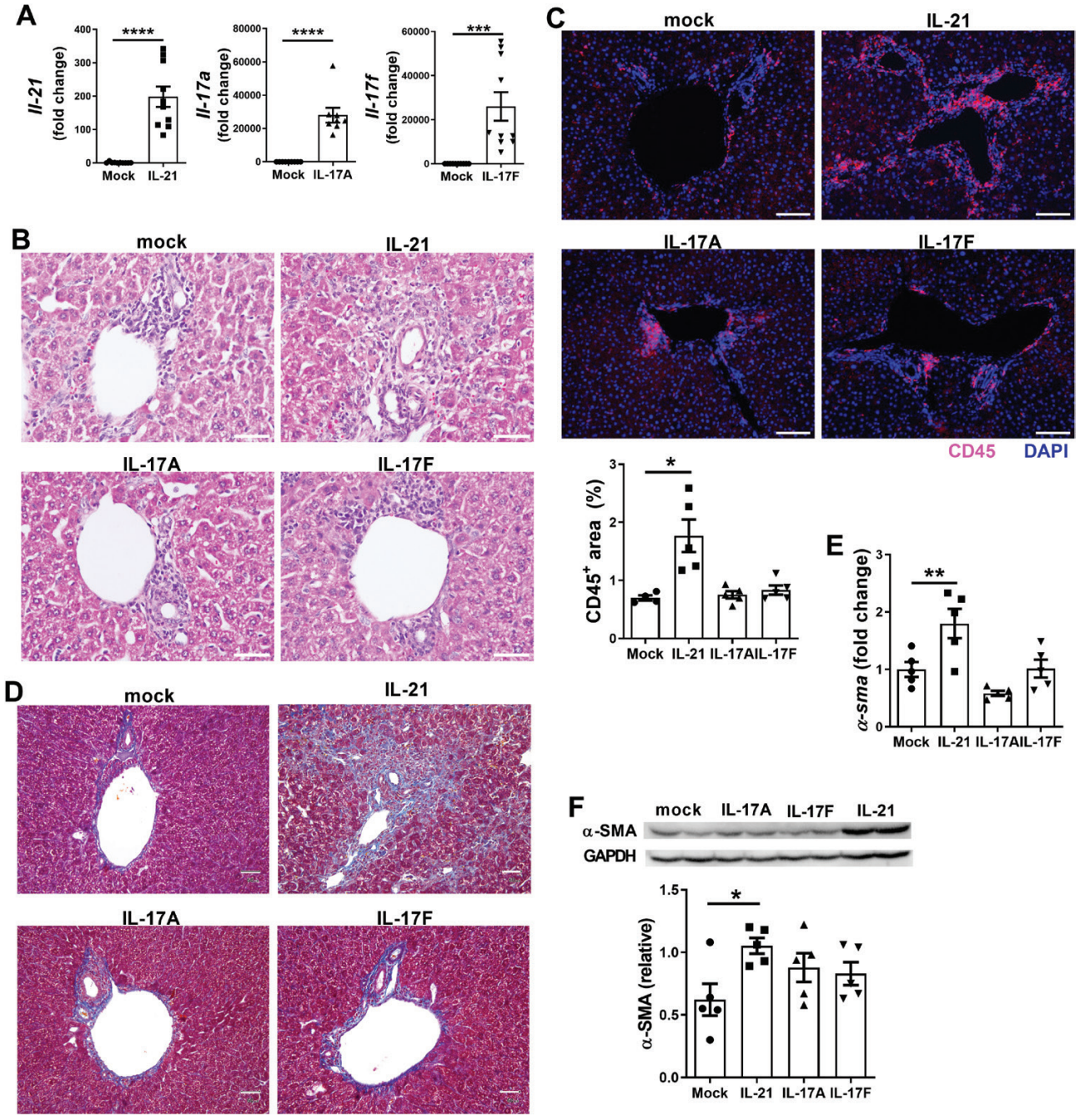

Figure 1. Effects on liver inflammation and fibrosis in autoimmune cholangitis mice treated with AAV-Th17 cytokines. Mice were injected with AAV-IL-17A, AAV-IL-17F, AAV-IL-21, or AAV-mock 2 weeks after the first 2-OA-OVA immunization and studied at week 11. (a) *Il17A*, *Il17F*, or *Il21* expressions in the liver were analyzed by RT-qPCR. (b) Representative H&E staining of liver sections. Scale bar, 30 μm. (c) Representative immunofluorescence staining (scale bar, 25 μm) and graphical summary of the $CD45^+$ fluorescence in the liver of all groups of mice. (d) Representative Masson's trichrome staining of liver sections. Scale bar, 50 μm. (e) The expressions of α-*Sma* mRNA in the liver were determined by RT-qPCR. (f) The expressions of α-SMA protein in the liver were determined by western blot and quantitation by ImageJ. Each dot represents an individual mouse. $n = 5–10$ mice per group. All error bars denote ± SEM. $^*P < 0.05$; $^{**}P < 0.01$; $^{***}P < 0.001$; $^{****}P < 0.0001$. Abbreviation: α-SMA: α-smooth muscle actin.

compared to the mock group (Fig. 2). However, we observed a significant decrease in *Cxcl10* expression in IL-17A-treated mice ($P < 0.05$; Fig. 2c). Anti-PDC-E2 IgG levels were increased in IL-21-treated mice compared to those in mock-treated control mice (Fig. 2a). *Ifn-γ* and *Tnf-α* levels were significantly increased in mice treated with IL-21 ($P < 0.01$; Fig. 2b). In addition, the expression of *Cxcl9* and *Cxcl10* in the livers of IL-21-treated mice was much higher than that in mock-treated control mice (Fig. 2c).

A marked increase in liver $CD8^+$T cells with active and memory phenotypes in IL-21-treated mice

Liver-infiltrated leukocytes were studied at 5 weeks post-2-OA-OVA immunization. Gating strategies for different subsets of lymphocytes by flow cytometry were shown in Fig. 3a. The overall numbers of the leukocyte and lymphocyte subsets in the liver of IL-17A- or IL-17F-treated mice remained unchanged compared to the mock-treated mice (Fig. 3b and d). The percentage of polymorphonuclear cells was elevated in

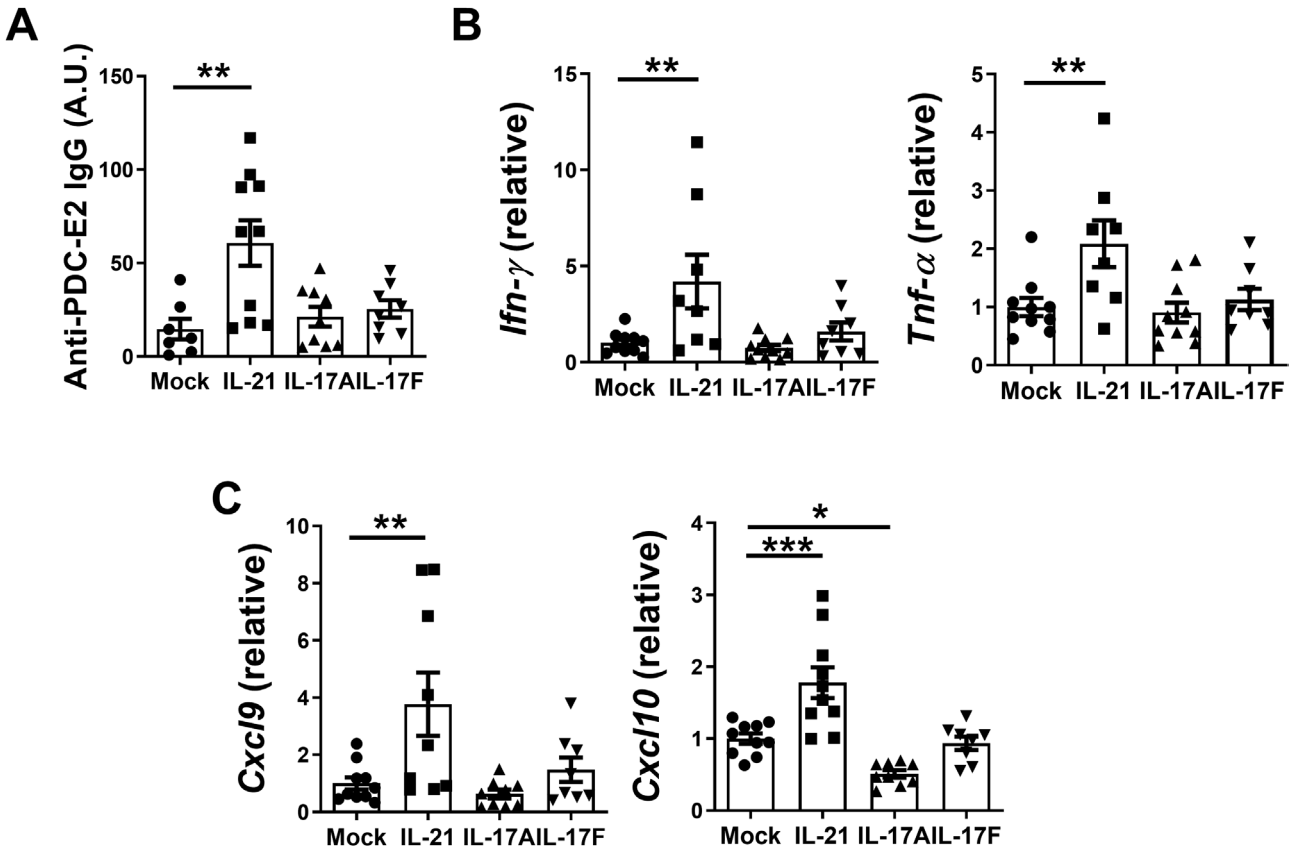

Figure 2. Effects on anti-PDC-E2 Abs and proinflammatory cytokines and chemokines in autoimmune cholangitis mice treated with AAV-Th17 cytokine. Mice were injected with AAV-IL-17A, AAV-IL-17F, AAV-IL-21, or AAV mock 2 weeks after the first 2-OA-OVA immunization and studied at week 5. (a) Serum levels of anti-PDC-E2 IgG were determined by ELISA. (b) The expressions of IFN-γ and TNF-α mRNA in the liver were determined by RT-qPCR. (c) The expressions of CXCL9 and CXCL10 mRNA in the liver were determined by RT-qPCR. Each dot represents an individual mouse. $n = 8–10$ mice per group. All error bars denote ±SEM. $^{*}P < 0.05$; $^{**}P < 0.01$; $^{***}P < 0.001$. Abbreviation: AU: arbitrary unit.

IL-17A-treated mice (Fig. 3c). IL-21-treated mice had more leukocyte infiltration in the liver with higher numbers of T cells and B cells (Fig. 3b and d). Both $CD4^+$ and $CD8^+$ T cell numbers were higher in IL-21-treated mice, but a higher ratio of CD8/CD4 was noted, indicating a higher $CD8^+$ T-cell infiltration relative to $CD4^+$ T cells in IL-21 treatment (Fig. 3e).

IFN-γ and granzyme B expression in liver $CD8^+$ T cells of AAV Th17 cytokine-administered mice were shown in Fig. 4a. The frequencies of IFN-γ-expressing $CD8^+$ T cells and granzyme B-expressing $CD8^+$ T cells were increased in IL-21-treated mice (Fig. 4b and c). Moreover, we observed a significant increase in FasL expression on $CD8^+$ T cells in the IL-21-treated group ($P < 0.05$; Fig. 4d). However, the liver $CD8^+$ T cells expressing IFN-γ, granzyme B, and/or FasL did not differ between IL-17A- or IL-17F-treated mice and the mock group (Fig. 4). The frequencies of IFN-γ-expressing $CD4^+$ T cells were no differences among four groups (Fig. 4e).

We also analyzed the liver memory T-cell subsets in cytokine-treated mice. Gating strategies for different subsets of memory T cells by flow cytometry were shown in Fig. 5a. As shown in Fig. 5b, mice treated with IL-21 had higher percentages and numbers of effector memory $CD4^+$ T cells (Tem). A lower percentage of tissue-resident memory $CD4^+$ T cells (Trm) were found in IL-21-treated mice. In contrast, the cell numbers were not different compared to mock controls (Fig. 5b). There were higher percentages and numbers of $CD8^+$ Trm cells in IL-21-treated mice compared to mock-treated mice. In addition, central memory (Tcm) and Tem $CD8^+$ cells in IL-21-treated mice were higher than in mock controls (Fig. 5c). The liver memory $CD4^+$ and $CD8^+$ T-cell subsets were not different in mice treated with either IL-17A or IL-17F compared to mock-treated mice (Fig. 5b and c).

Lower Th1 cells and higher $CD11b^+Ly6G^+$ cells in the livers of autoimmune cholangitis mice treated with AAV-IL-17

Although there were no apparent changes in liver inflammation in mice treated with IL-17A, correlation analysis demonstrated that the numbers of lymphocytes, $CD4^+$ T cells, and $CD8^+$ T cells in the liver were negatively correlated with serum levels of IL-17A ($r = –0.66$, $P = 0.04$; $r = –0.75$, $P = 0.02$; and $r = –0.75$, $P = 0.02$, respectively; Fig. 6a). There was a significantly lower percentage of IFN-γ-producing $CD4^+$ T cells in IL-17A-treated mice than in the mock-treated mice ($P < 0.05$). However, there was no difference in the percentage of IL-17A-producing $CD4^+$ T cells between IL-17A-treated and mock-treated mice (Fig. 6b). Notably, polymorphonuclear cell numbers were significantly higher in the livers of IL-17A-treated mice ($P < 0.001$; Fig. 6c). In addition, $CD3^-CD19^-NK1.1^-CD11b^+Ly6G^+$ cell numbers in the liver were higher in IL-17A-treated mice (Fig. 6d). Altogether, IL-17A decreased Th1 cells and increased $CD3^-CD19^-NK1.1^-CD11b^+Ly6G^+$ cells in the liver of mice with autoimmune cholangitis.

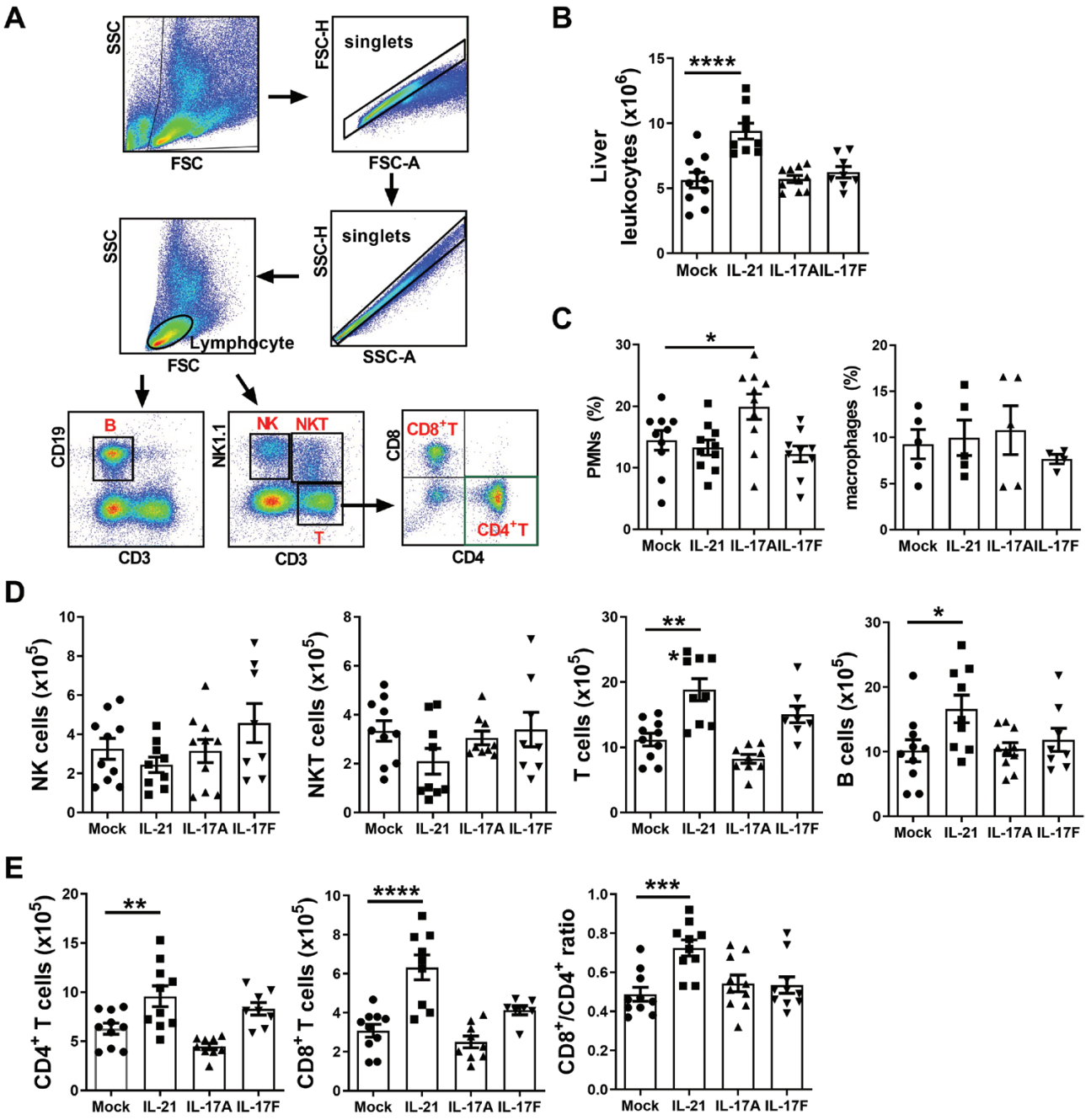

Figure 3. Effects on immune cell recruitment in autoimmune cholangitis mice treated with AAV-Th17 cytokines. Mice were injected with AAV-IL-17A, AAV-IL-17F, AAV-IL-21, or AAV mock 2 weeks after the first 2-OA-OVA immunization and studied at week 5. (a) Representative flow plots show gating strategies for different subsets of lymphocytes. (b) Liver leukocytes were quantified. (c) The percentages of polymorphonuclear cells (PMNs) and macrophages were determined. PMNs are $CD3^-CD19^-NK1.1^-CD11b^+Ly6G^+$. Macrophages are $CD3^-CD19^-NK1.1^-$ $F4/80^+CD11b^+$. (d) The numbers of NK, NKT, T, and B cells in the liver were quantified. (e) The numbers of $CD4^+$ and $CD8^+$ T cells and the ratios of $CD8^+/CD4^+$ T cells in the liver were assayed. Each dot represents an individual mouse. $n = 8–10$ mice per group. All error bars denote ±SEM. $^*P < 0.05$; $^{**}P < 0.01$; $^{***}P < 0.001$; $^{****}P < 0.0001$.

Discussion

In this study, we over-expressed IL-17A, IL-17F, or IL-21 in the liver of autoimmune cholangitis mice to investigate whether and how IL-17A, IL-17F, and IL-21 were involved in the pathogenesis of PBC. Our results demonstrated that administering IL-17A and IL-17F had little to no effect on liver inflammation and fibrosis. However, administering IL-21 enhanced the liver inflammatory response and immune cell infiltration. Moreover, liver fibrosis was augmented in IL-21-treated mice.

IL-17A is the main cytokine produced by Th17 cells. In PBC patients, there is an increase in the serum levels of IL-17A and $IL-17A^+$ cell numbers in the portal area, especially in the advanced stage of the disease [6–8]. The levels of AMAs and portal inflammation are reduced in IL-17A knockout PBC mice [29], suggesting a pathogenic role of IL-17A in PBC. However, it has been demonstrated that the deletion of IL-17A in IL-2R$\alpha^{-/-}$ mice caused autoimmune cholangitis, leading to more severe liver inflammation, suggesting the protective role of IL-17A [30]. This study showed

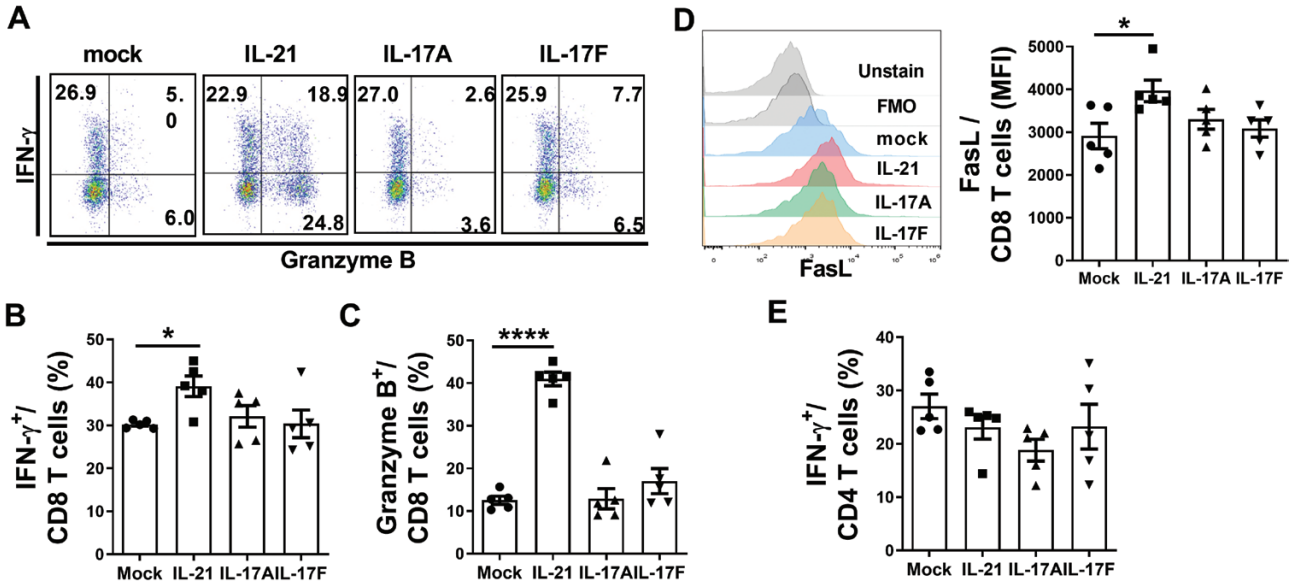

Figure 4. Effects on the activity of CD8⁺ T cells in autoimmune cholangitis mice treated with AAV-Th17 cytokines. Mice were injected with AAV-IL-17A, AAV-IL-17F, AAV-IL-21, or AAV mock 2 weeks after the first 2-OA-OVA immunization and studied at week 5. (a) Representative flow plots show IFN-γ and granzyme B expression in liver CD8⁺ T cells of AAV Th17 cytokine-administered mice. Numbers in quadrants indicate the percent cells in each. (b) The percentages of IFN-γ expressing CD8⁺ T cells were quantified. (c) The percentages of granzyme B expressing CD8⁺ T cells were quantified. (d) Representative flow cytometry analysis and graphical summary of mean fluorescence intensity (MFI) of FasL expression on liver CD8⁺ T cells of AAV Th17 cytokine administered mice. FMO, fluorescence minus one, controls are the experimental cells stained with all the fluorophores minus one fluorophore. (e) The percentages of IFN-γ expressing CD4⁺ T cells were quantified. Each dot represents an individual mouse. $n = 5$ mice per group. All error bars denote ±SEM. *$P < 0.05$; ****$P < 0.0001$.

no noticeable increase in AMAs, number and function of infiltrated immune cells, liver inflammation, and fibrosis in IL-17-treated autoimmune cholangitis mice. Notably, we found IFN-γ-secreting Th1 cells were lower in IL-17A-treated mice. There was a negative correlation between cell infiltration and serum IL-17A levels. In addition, there was a significant increase in the number of $CD3^-CD19^-NK1.1^-CD11b^+Ly6G^+$ cells detected on week 5, which may be polymorphonuclear myeloid-derived suppressor cells (PMN-MDSCs) after IL-17 treatment. MDSCs are a population of myeloid cells with potent immunosuppressive activity. In contrast to neutrophils in acute infection or inflammation, they are generated under persistent stimulation associated with chronic infection or inflammation involving relatively low-strength signals [31]. Reportedly, IL-17A can induce and regulate MDSCs, suppress anti-tumor immune responses, and promote tumor development [32]. These results suggest that IL-17 does not enhance but mildly reduces inflammation in autoimmune cholangitis.

IL-17F shares 50% amino acid identity and binds to the same receptor as IL-17A [10]. IL-17F is less efficient at signaling through IL-17R than IL-17A, but the previous study showed that the downstream activities of IL-17F are similar to those of IL-17A [33]. It has been shown that increased IL-17F is more clinically relevant than IL-17A in primary Sjögren's syndrome [34], indicating that IL-17A and IL-17F have overlapping yet distinct functions in autoimmune diseases. However, in our study, IL-17F does not affect autoimmune cholangitis.

In patients with PBC, the serum levels of IL-21 are significantly higher [35]. Variants of IL-21 and IL-21 receptor (IL-21R) are identified as risk loci for PBC in a genome-wide association study [36]. Enhanced expression of IL-21 and IL-21R in the hepatic portal tracks of PBC livers is observed. Furthermore, the numbers of IL-21⁺ and IL-21R⁺ cells positively correlate with inflammation severity and stages of hepatic fibrosis [36]. IL-21 enhanced liver inflammation and liver fibrosis in mice with autoimmune cholangitis, revealing the role of IL-21 in the pathogenesis of PBC. In line with a previous study showing that IL-21 induces the expression of cytotoxic molecules and promotes CD8 T-cell cytotoxicity [37], our model mice treated with IL-21 had increased numbers of CD8⁺ T cells with cytotoxic molecules and memory phenotype. Moreover, we noted an increased IFN-γ production in the liver and increased IFN-γ-producing CD8⁺ T cells. Previously, we demonstrated that IFN-γ is important in initiating autoimmune cholangitis, increasing lymphocyte infiltration, and enhancing inflammation [24]. Altogether, IL-21 exacerbates the severity of autoimmune cholangitis by increasing the number and effector cytotoxic function of CD8⁺ T cells and inducing IFN-γ expression to skew the liver microenvironment to promote Th1 conditions.

Trm cells, a recently described population, do not recirculate like Tcm and Tem cells but remain localized within specific tissues, including the liver [38, 39]. In addition to their rapid on-site immune protection against previously exposed pathogens in peripheral tissues [38, 39], evidence suggests that autoreactive and/or aberrantly activated Trm cells may be involved in the pathogenesis of autoimmune diseases, such as psoriasis, multiple sclerosis, type 1 diabetes, and rheumatoid arthritis [40–42]. Autoimmune cholangitis mice treated with IL-21 showed severe liver inflammation, fibrosis, and increased liver CD8⁺ Trm cells, suggesting a role of CD8⁺ Trm in PBC. Reportedly, IL-21 promotes brain CD8 Trm differentiation during persistent viral infection [43].

This study found increased AMA IgG in autoimmune cholangitis mice treated with IL-21. Using a $p40^{-/-}$IL-2Rα$^{-/-}$ PBC

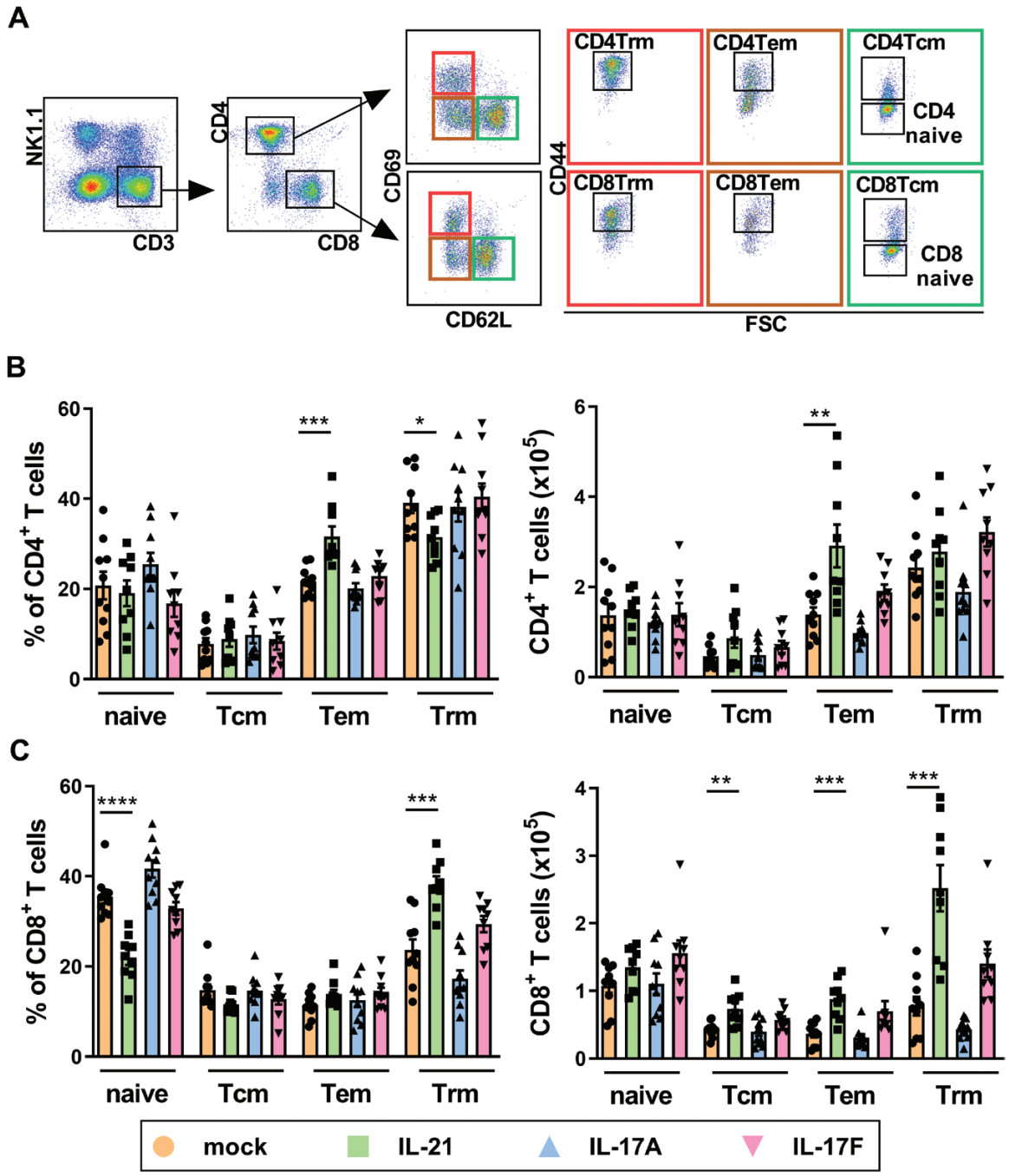

Figure 5. Increased resident memory CD8⁺ T cells in autoimmune cholangitis mice treated with AAV-IL-21. Mice were injected with AAV-IL-17A, AAV-IL-17F, AAV-IL-21, or AAV mock 2 weeks after the first 2-OA-OVA immunization and studied at week 5. (a) Representative flow plots show gating strategies for different subsets of lymphocytes. (b) The percentages and numbers of naïve, Tcm, Tem, and Trm CD4⁺ T cells. (c) The percentages and numbers of naïve, Tcm, Tem, and Trm CD8⁺ T cells. Each dot represents an individual mouse. $n = 8$–10 mice per group. All error bars denote ±SEM. *$P < 0.05$; ***$P < 0.001$; ****$P < 0.0001$. Tcm: central memory T; Tem: effector memory T; Trm: tissue-resident memory T. Abbreviations: Naïve T: $CD62L^+CD69^-CD44^-$; Tcm: $CD62L^+CD69^-CD44^+$; Tem: $CD62L^-CD69^-CD44^+$; Trm: $CD62L^-CD69^+CD44^+$.

mouse model, Wu et al. find that deficiency of IL-21 results in the significant downregulation of AMAs [44]. These results suggest that IL-21 is critical in AMA production. The role of IL-21 in T-cell-dependent B-cell responses has been well documented [45]. IL-21 regulates the interaction between follicular helper T cells and germinal center B cells for antibody production [46]. We found that IL-21-treated mice had higher numbers of B cells and anti-PDC-E2 antibodies. Anti-PDC-E2 antibodies react with the antigenically reactive form of PDC-E2 in apoptotic blebs from apoptotic biliary epithelial cells and activate innate immune responses. The apotope–autoantibody complex stimulates macrophages and induces a localized burst of proinflammatory cytokines [47]. However, whether anti-PDC-E2 antibody plays a role in liver fibrosis remains unclear.

We observed apparent liver fibrosis in IL-21-treated mice. We also observed increased levels of α-SMA in the liver. α-SMA is expressed by HSC, which reflects their activation

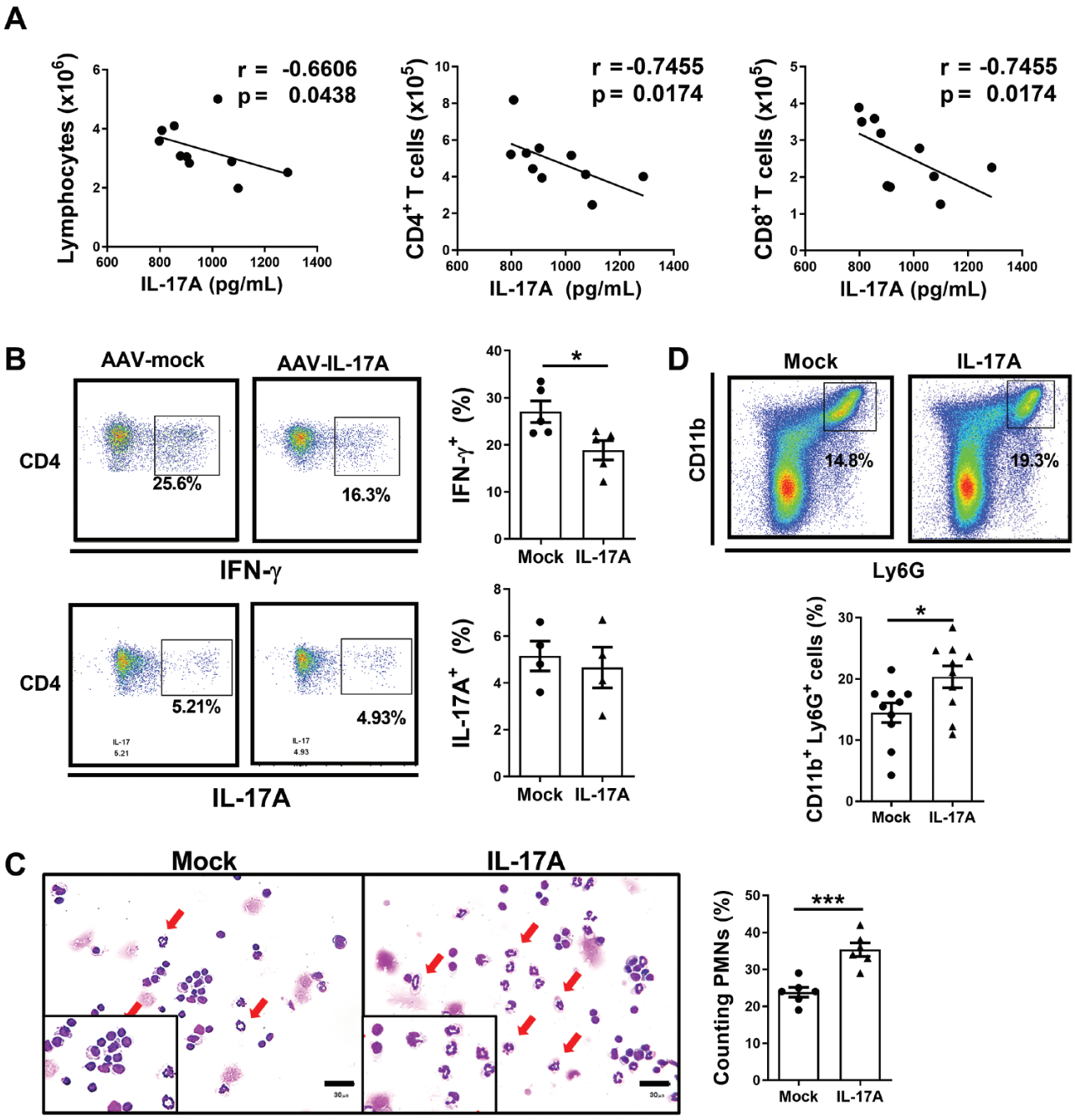

Figure 6. Decreased Th1 levels and increased CD11b⁺Ly6G⁺ levels in the liver of autoimmune cholangitis mice treated with AAV-IL-17. Mice were injected with AAV-IL-17 or AAV mock 2 weeks after the first 2-OA-OVA immunization and studied at week 5. (a) The relationship between the serum levels of IL-17 and the numbers of lymphocytes, CD4⁺ T cells, and CD8⁺ T cells in the IL-17-treated 2-OA-OVA immunized mice. (b) Representative dot plots and graphical summary of IFN-γ expressing CD4⁺ T cells and IL-17A expressing CD4⁺ T cells in the liver of mock and IL-17-treated PBC mice. (c) Liver leukocytes from AAV-mock and AAV-IL-17 injected PBC mice were subjected to cytospin centrifugation and staining. Polymorphonuclear cells (PMN) were indicated with an arrow. The percentages of PMN were scored. (d) Representative dot plots and graphical summary of Ly6G⁺ CD11b⁺ cells (gated on CD3⁻CD19⁻NK1.1⁻ cells) in the liver of mock and IL-17-treated mice. Each dot represents an individual mouse. n = 4–10 mice per group. All error bars denote ±SEM. *$P < 0.05$; ***$P < 0.001$.

to myofibroblast-like cells. HSCs are located in the space of the Disse of the liver. Upon activation to be myofibroblast-like cells, they produce large amounts of collagen, driving liver fibrogenesis [48]. In addition to immune cells, HSCs and LX-2 cell lines (immortalized human HSCs) also express the IL-21R. Adding IL-21 upregulates the expression of α-SMA in LX-2 cells [49, 50]. Reportedly, IL-21 promotes lung fibrosis by introducing a novel population of IL-13-producing CD8⁺ T cells in a bleomycin-treated lung injury model [51]. In our liver-disease model, we found that administration of IL-21 induced a robust increase in CD8⁺ T cells but not the profibrotic cytokines IL-4 and IL-13. Although much work remains to be done, we propose that IL-21 could promote HSC activation directly or through the induction of CD8⁺ T cells, resulting in hepatic fibrosis in autoimmune cholangitis.

IL-17A, the primary cytokine produced by Th17 cells, has been linked to the involvement of 'Th17 cells' in PBC based on studies detecting IL-17A-expressing cells within the Th17 subset [5–9]. However, Th17 cells can secrete multiple effector cytokines, such as IL-17F, IL-21, and IL-22 [3, 4], complicating the understanding their role in PBC. Our current study provides new insights. Contrary to previous assumptions, we found that the administration of IL-17A did not exacerbate inflammation but instead led to a mild reduction in autoimmune cholangitis. Intriguingly, our results indicate that IL-21, another effector cytokine secreted by Th17 cells, played a pivotal role. Its administration resulted in a significant enhancement of liver inflammation and fibrosis in the context of autoimmune cholangitis. In summary, our findings suggest that while IL-17A is a characteristic cytokine produced by Th17 cells, it may not be the critical mediator driving PBC pathogenesis. Instead, our data highlight the significance of IL-21 as the effector of Th17 cell-derived cytokine in this context. However, it is important to acknowledge that our experimental approach primarily addresses the influence of Th17 cell-derived cytokines on PBC pathogenesis without directly investigating the involvement of Th17 cells themselves in this scenario. Future studies should delve into an in-depth analysis of intrahepatic IL-17A, IL-17F, and IL-21-expressing cell populations.

Acknowledgments

We thank Pi-Hui Liang at the National Taiwan University for technical assistance in preparing 2-OA-OVA. We thank Tiffany E. Wu for technical support.

Funding

This work was supported by grants from the Career Development Project of National Taiwan University (104R7880, 105R7880), the Excellent Translational Medicine Research Projects of National Taiwan University College of Medicine and National Taiwan University Hospital (NSCCMOH-94-6, NSCCMOH-131-8), the Ministry of Science and Technology, Taiwan (MOST 108-2320-B-002-052-MY3) and the National Health Research Institutes, Taiwan (NHRI-EX110-11028SI; NHRI-EX111-11028SI).

Conflict of Interest

The authors declare no competing financial interests.

Author Contributions

Conceptualization: Y.-H. C.; Methodology: C.-W. C., H.-W. C., Y.-W. W., C.-I. L., and Y.-H. C.; Investigation: C.-W. C., H.-W. C., Y.-W. W., C.-I. L., and Y.-H. C.; Writing—Original Draft: C.-W. C. and Y.-H. C.; Writing—Review and editing: Y.-H. C.; Funding acquisition: Y.-H. C.; Supervision: Y.-H. C.

Data Availability

Data are available on reasonable request.

References

1. Hirschfield GM, Gershwin ME. The immunobiology and pathophysiology of primary biliary cirrhosis. *Annu Rev Pathol* 2013, 8, 303–30. doi:10.1146/annurev-pathol-020712-164014
2. Lleo A, Leung PSC, Hirschfield GM, Gershwin EM. The pathogenesis of primary biliary cholangitis: a comprehensive review. *Semin Liver Dis* 2020, 40, 34–48.
3. Park H, Li Z, Yang XO, Chang SH, Nurieva R, Wang YH, et al. A distinct lineage of CD4 T cells regulates tissue inflammation by producing interleukin 17. *Nat Immunol* 2005, 6, 1133–41. doi:10.1038/ni1261
4. Ouyang W, Kolls JK, Zheng Y. The biological functions of T helper 17 cell effector cytokines in inflammation. *Immunity* 2008, 28, 454–67. doi:10.1016/j.immuni.2008.03.004
5. Harada K, Shimoda S, Sato Y, Isse K, Ikeda H, Nakanuma Y. Periductal interleukin-17 production in association with biliary innate immunity contributes to the pathogenesis of cholangiopathy in primary biliary cirrhosis. *Clin Exp Immunol* 2009, 157, 261–70. doi:10.1111/j.1365-2249.2009.03947.x
6. Lan RY, Salunga TL, Tsuneyama K, Lian ZX, Yang GX, Hsu W, et al. Hepatic IL-17 responses in human and murine primary biliary cirrhosis. *J Autoimmun* 2009, 32, 43–51. doi:10.1016/j.jaut.2008.11.001
7. Shi T, Zhang T, Zhang L, Yang Y, Zhang H, Zhang F. The distribution and the fibrotic role of elevated inflammatory Th17 cells in patients with primary biliary cirrhosis. *Medicine (Baltim)* 2015, 94, e1888. doi:10.1097/MD.0000000000001888
8. Rong G, Zhou Y, Xiong Y, Zhou L, Geng H, Jiang T, et al. Imbalance between T helper type 17 and T regulatory cells in patients with primary biliary cirrhosis: the serum cytokine profile and peripheral cell population. *Clin Exp Immunol* 2009, 156, 217–25. doi:10.1111/j.1365-2249.2009.03898.x
9. Yang CY, Ma X, Tsuneyama K, Huang S, Takahashi T, Chalasani NP, et al. IL-12/Th1 and IL-23/Th17 biliary microenvironment in primary biliary cirrhosis: implications for therapy. *Hepatology* 2014, 59, 1944–53. doi:10.1002/hep.26979
10. Maddur MS, Miossec P, Kaveri SV, Bayry J. Th17 cells: biology, pathogenesis of autoimmune and inflammatory diseases, and therapeutic strategies. *Am J Pathol* 2012, 181, 8–18. doi:10.1016/j.ajpath.2012.03.044
11. Hot A, Miossec P. Effects of interleukin (IL)-17A and IL-17F in human rheumatoid arthritis synoviocytes. *Ann Rheum Dis* 2011, 70, 727–32. doi:10.1136/ard.2010.143768
12. Tang C, Kakuta S, Shimizu K, Kadoki M, Kamiya T, Shimazu T, et al. Suppression of IL-17F, but not of IL-17A, provides protection against colitis by inducing Treg cells through modification of the intestinal microbiota. *Nat Immunol* 2018, 19, 755–65. doi:10.1038/s41590-018-0134-y
13. Corneth OB, Mus AM, Asmawidjaja PS, Klein Wolterink RG, van Nimwegen M, Brem MD, et al. Absence of interleukin-17 receptor a signaling prevents autoimmune inflammation of the joint and leads to a Th2-like phenotype in collagen-induced arthritis. *Arthritis Rheumatol* 2014, 66, 340–9. doi:10.1002/art.38229
14. Wilson MS, Madala SK, Ramalingam TR, Gochuico BR, Rosas IO, Cheever AW, et al. Bleomycin and IL-1beta-mediated pulmonary fibrosis is IL-17A dependent. *J Exp Med* 2010, 207, 535–52. doi:10.1084/jem.20092121
15. Tan Z, Qian X, Jiang R, Liu Q, Wang Y, Chen C, et al. IL-17A plays a critical role in the pathogenesis of liver fibrosis through hepatic stellate cell activation. *J Immunol* 2013, 191, 1835–44. doi:10.4049/jimmunol.1203013
16. Meng F, Wang K, Aoyama T, Grivennikov SI, Paik Y, Scholten D, et al. Interleukin-17 signaling in inflammatory, Kupffer cells, and hepatic stellate cells exacerbates liver fibrosis in mice. *Gastroenterology* 2012, 143, 765–776.e3. doi:10.1053/j.gastro.2012.05.049
17. Fabre T, Kared H, Friedman SL, Shoukry NH. IL-17A enhances the expression of profibrotic genes through upregulation of the TGF-beta receptor on hepatic stellate cells in a JNK-dependent manner. *J Immunol* 2014, 193, 3925–33. doi:10.4049/jimmunol.1400861
18. Spolski R, Leonard WJ. Interleukin-21: a double-edged sword with therapeutic potential. *Nat Rev Drug Discov* 2014, 13, 379–95. doi:10.1038/nrd4296
19. Korn T, Bettelli E, Gao W, Awasthi A, Jager A, Strom TB, et al. IL-21 initiates an alternative pathway to induce proinflammatory T(H)17 cells. *Nature* 2007, 448, 484–7. doi:10.1038/nature05970

20. Zeng R, Spolski R, Finkelstein SE, Oh S, Kovanen PE, Hinrichs CS, et al. Synergy of IL-21 and IL-15 in regulating CD8+ T cell expansion and function. *J Exp Med* 2005, 201, 139–48. doi:10.1084/jem.20041057
21. Konforte D, Simard N, Paige CJ. IL-21: an executor of B cell fate. *J Immunol* 2009, 182, 1781–7. doi:10.4049/jimmunol.0803009
22. Dudakov JA, Hanash AM, van den Brink MRM. Interleukin-22: immunobiology and pathology. *Annu Rev Immunol* 2015, 33, 747–85. doi:10.1146/annurev-immunol-032414-112123
23. Hsueh YH, Chang YN, Loh CE, Gershwin ME, Chuang YH. AAV-IL-22 modifies liver chemokine activity and ameliorates portal inflammation in murine autoimmune cholangitis. *J Autoimmun* 2016, 66, 89–97. doi:10.1016/j.jaut.2015.10.005
24. Syu BJ, Loh CE, Hsueh YH, Gershwin ME, Chuang YH. Dual roles of IFN-gamma and IL-4 in the natural history of murine autoimmune cholangitis: IL-30 and implications for precision medicine. *Sci Rep* 2016, 6, 34884. doi:10.1038/srep34884
25. Hsueh YH, Chen HW, Syu BJ, Lin CI, Leung PSC, Gershwin ME, et al. Endogenous IL-10 maintains immune tolerance but IL-10 gene transfer exacerbates autoimmune cholangitis. *J Autoimmun* 2018, 95, 159–70. doi:10.1016/j.jaut.2018.09.009
26. Wu SJ, Yang YH, Tsuneyama K, Leung PS, Illarionov P, Gershwin ME, et al. Innate immunity and primary biliary cirrhosis: activated invariant natural killer T cells exacerbate murine autoimmune cholangitis and fibrosis. *Hepatology* 2011, 53, 915–25. doi:10.1002/hep.24113
27. Grimm D, Lee JS, Wang L, Desai T, Akache B, Storm TA, et al. In vitro and in vivo gene therapy vector evolution via multispecies interbreeding and retargeting of adeno-associated viruses. *J Virol* 2008, 82, 5887–911. doi:10.1128/JVI.00254-08
28. Wang YW, Lin CI, Chen HW, Wu JC, Chuang YH. Apoptotic biliary epithelial cells and gut dysbiosis in the induction of murine primary biliary cholangitis. *J Transl Autoimmun* 2023, 6, 100182. doi:10.1016/j.jtauto.2022.100182
29. Kawata K, Tsuda M, Yang GX, Zhang W, Tanaka H, Tsuneyama K, et al. Identification of potential cytokine pathways for therapeutic intervention in murine primary biliary cirrhosis. *PLoS One* 2013, 8, e74225. doi:10.1371/journal.pone.0074225
30. Yang W, Yao Y, Yang YQ, Lu FT, Li L, Wang YH, et al. Differential modulation by IL-17A of cholangitis versus colitis in IL-2Ralpha deleted mice. *PLoS One* 2014, 9, e105351. doi:10.1371/journal.pone.0105351
31. Gabrilovich DI. Myeloid-derived suppressor cells. *Cancer Immunol Res* 2017, 5, 3–8. doi:10.1158/2326-6066.CIR-16-0297
32. He D, Li H, Yusuf N, Elmets CA, Li J, Mountz JD, et al. IL-17 promotes tumor development through the induction of tumor promoting microenvironments at tumor sites and myeloid-derived suppressor cells. *J Immunol* 2010, 184, 2281–8. doi:10.4049/jimmunol.0902574
33. Yang XO, Chang SH, Park H, Nurieva R, Shah B, Acero L, et al. Regulation of inflammatory responses by IL-17F. *J Exp Med* 2008, 205, 1063–75. doi:10.1084/jem.20071978
34. Gan Y, Zhao X, He J, Liu X, Li Y, Sun X, et al. Increased interleukin-17F is associated with elevated autoantibody levels and more clinically relevant than interleukin-17A in primary Sjogren's syndrome. *J Immunol Res* 2017, 2017, 4768408. doi:10.1155/2017/4768408
35. Wang L, Sun X, Qiu J, Cai Y, Ma L, Zhao P, et al. Increased numbers of circulating ICOS(+) follicular helper T and CD38(+) plasma cells in patients with newly diagnosed primary biliary cirrhosis. *Dig Dis Sci* 2015, 60, 405–13. doi:10.1007/s10620-014-3372-3
36. Qiu F, Tang R, Zuo X, Shi X, Wei Y, Zheng X, et al. A genome-wide association study identifies six novel risk loci for primary biliary cholangitis. *Nat Commun* 2017, 8, 14828. doi:10.1038/ncomms14828
37. Sutherland AP, Joller N, Michaud M, Liu SM, Kuchroo VK, Grusby MJ. IL-21 promotes CD8+ CTL activity via the transcription factor T-bet. *J Immunol* 2013, 190, 3977–84. doi:10.4049/jimmunol.1201730
38. Fernandez-Ruiz D, Ng WY, Holz LE, Ma JZ, Zaid A, Wong YC, et al. Liver-resident memory CD8(+) T cells form a front-line defense against malaria liver-stage infection. *Immunity* 2016, 45, 889–902. doi:10.1016/j.immuni.2016.08.011
39. Tse SW, Radtke AJ, Espinosa DA, Cockburn IA, Zavala F. The chemokine receptor CXCR6 is required for the maintenance of liver memory CD8(+) T cells specific for infectious pathogens. *J Infect Dis* 2014, 210, 1508–16. doi:10.1093/infdis/jiu281
40. Suarez-Farinas M, Fuentes-Duculan J, Lowes MA, Krueger JG. Resolved psoriasis lesions retain expression of a subset of disease-related genes. *J Invest Dermatol* 2011, 131, 391–400. doi:10.1038/jid.2010.280
41. Sasaki K, Bean A, Shah S, Schutten E, Huseby PG, Peters B, et al. Relapsing-remitting central nervous system autoimmunity mediated by GFAP-specific CD8 T cells. *J Immunol* 2014, 192, 3029–42. doi:10.4049/jimmunol.1302911
42. Kuric E, Seiron P, Krogvold L, Edwin B, Buanes T, Hanssen KF, et al. Demonstration of tissue resident memory CD8 T cells in insulitic lesions in adult patients with recent-onset type 1 diabetes. *Am J Pathol* 2017, 187, 581–8. doi:10.1016/j.ajpath.2016.11.002
43. Ren HM, Kolawole EM, Ren M, Jin G, Netherby-Winslow CS, Wade Q, Shwetank, Rahman ZSM, Evavold BD, Lukacher AE. IL-21 from high-affinity CD4 T cells drives differentiation of brain-resident CD8 T cells during persistent viral infection. *Sci Immunol* 2020, 5, eabb5590.
44. Xu YF, Yao Y, Ma M, Yang SH, Jiang P, Wang J, et al. The proinflammatory cytokines IL-18, IL-21, and IFN-gamma differentially regulate liver inflammation and anti-mitochondrial antibody level in a murine model of primary biliary cholangitis. *J Immunol Res* 2022, 2022, 7111445. doi:10.1155/2022/7111445
45. Ozaki K, Spolski R, Ettinger R, Kim HP, Wang G, Qi CF, et al. Regulation of B cell differentiation and plasma cell generation by IL-21, a novel inducer of Blimp-1 and Bcl-6. *J Immunol* 2004, 173, 5361–71. doi:10.4049/jimmunol.173.9.5361
46. Luthje K, Kallies A, Shimohakamada Y, Belz GT, Light A, Tarlinton DM, et al. The development and fate of follicular helper T cells defined by an IL-21 reporter mouse. *Nat Immunol* 2012, 13, 491–8. doi:10.1038/ni.2261
47. Lleo A, Bowlus CL, Yang GX, Invernizzi P, Podda M, Van de Water J, et al. Biliary apotopes and anti-mitochondrial antibodies activate innate immune responses in primary biliary cirrhosis. *Hepatology* 2010, 52, 987–98. doi:10.1002/hep.23783
48. Hernandez-Gea V, Friedman SL. Pathogenesis of liver fibrosis. *Annu Rev Pathol* 2011, 6, 425–56. doi:10.1146/annurev-pathol-011110-130246
49. Wang Y, Lin C, Cao Y, Duan Z, Guan Z, Xu J, et al. Up-regulation of interleukin-21 contributes to liver pathology of schistosomiasis by driving GC immune responses and activating HSCs in mice. *Sci Rep* 2017, 7, 16682. doi:10.1038/s41598-017-16783-7
50. Feng G, Zhang JY, Zeng QL, Yu X, Zhang Z, Lv S, et al. Interleukin-21 mediates hepatitis B virus-associated liver cirrhosis by activating hepatic stellate cells. *Hepatol Res* 2014, 44, E198–205. doi:10.1111/hepr.12215
51. Brodeur TY, Robidoux TE, Weinstein JS, Craft J, Swain SL, Marshak-Rothstein A. IL-21 promotes pulmonary fibrosis through the induction of profibrotic CD8+ T cells. *J Immunol* 2015, 195, 5251–60. doi:10.4049/jimmunol.1500777